

# Theory of Hantavirus Infection Spread Incorporating Localized Adult and Itinerant Juvenile Mice

V. M. Kenkre,<sup>1</sup> L. Giuggioli,<sup>1</sup> G. Abramson,<sup>1,2</sup> and G. Camelo-Neto<sup>1</sup>

<sup>1</sup>*Consortium of the Americas for Interdisciplinary Science and Department of Physics and Astronomy,  
University of New Mexico, Albuquerque, New Mexico 87131, USA*

<sup>2</sup>*Centro Atómico Bariloche, CONICET and Instituto Balseiro,  
8400 San Carlos de Bariloche, Río Negro, Argentina.*

(Dated: October 26, 2018)

A generalized model of the spread of the Hantavirus in mice populations is presented on the basis of recent observational findings concerning the movement characteristics of the mice that carry the infection. The factual information behind the generalization is based on mark-recapture observations reported in Giuggioli et al. [Bull. Math. Biol. **67** 1135 (2005)] that have necessitated the introduction of home ranges in the simple model of Hantavirus spread presented by Abramson and Kenkre [Phys. Rev. E **66** 11912 (2002)]. The essential feature of the model presented here is the existence of adult mice that remain largely confined to locations near their home ranges, and itinerant juvenile mice that are not so confined, and, during their search for their own homes, move and infect both other juveniles and adults that they meet during their movement. The model is presented at three levels of description: mean field, kinetic and configuration. Results of calculations are shown explicitly from the mean field equations and the simulation rules, and are found to agree in some respects and to differ in others. The origin of the differences is shown to lie in spatial correlations. It is indicated how mark-recapture observations in the field may be employed to verify the applicability of the theory.

PACS numbers: 87.19.Xx, 87.23.Cc, 05.45.-a

## I. BACKGROUND AND MOTIVATION FOR THE STUDY

The spread of epidemics is an important topic that has received a great deal of attention from researchers in recent times [1, 2, 3, 4, 5, 6]. This interest stems from multiple factors. On the utilitarian side, concerns regarding human health provide an obvious reason for carrying out such studies. An equally important motivation arises purely from intellectual sources: the desire to gain a general understanding of spatially resolved strongly interacting systems on a macroscopic scale. Examples of epidemics of particular interest to the interdisciplinary scientist are the plague, the West Nile virus, and the Hantavirus. From the many-body aspect in (theoretical) modeling activities, the first presents formidable problems related to the number of carriers and diverse interactions of the fleas and their connections to their hosts. The second provides an interesting example of a system with two carriers, mosquitoes and birds, with disparate lifespans (weeks and years respectively) and suggests [7] time scale disparity analyses known in condensed matter sciences (see e.g. a discussion of the Born-Oppenheimer approximation in solids in ref. [8]). The simplest of the epidemics to study, from the conceptual viewpoint of a theorist, is the Hantavirus [1, 2, 3, 4, 5, 6]. It is the subject of the study presented below.

The details of the Hantavirus epidemic may be found in the review by Yates et al. [1] and related refs. [2, 3, 4, 5, 6]. The essential feature of the epidemic from the modeling point of view is that the infection is carried by mice that move from one physical location to another, and is transmitted to other mice through what are probably aggressive encounters. It is believed that the mice and the virus have coexisted for millions of years and therefore the mice do not die, nor are otherwise impaired, from contraction of the virus. This feature is peculiar to the Hantavirus and not shared with other epidemics such as the plague or the West Nile virus where the carriers may die from contracting the virus. Oscillations in the population which are characteristic of such behavior are therefore absent in the Hantavirus. Furthermore, in the Hantavirus context, no mice are born infected: infection may only be contracted from other mice after birth: there is no “vertical transmission” of the disease. The human population is incidental to the evolution of infection within the mouse population since humans get the virus from the mice but have no feedback effects on the mice in the infection process.

These features of the epidemic led a few years ago to the construction by two of the present authors of a simple model of the spread of the Hantavirus in the mouse population. In addition to the above features particular to the epidemic, interaction of the mice with the environment through standard logistic terms [9, 10] and motion of the mice over the terrain viewed as a simple and free random walk were the elements that went into the making of the model. The model was introduced at the usual three levels of the description of a many-body system: the most crude, the mean field level, the more detailed, the kinetic level, and the most detailed, the configuration level. The last was handled through simulations [11]. The first two levels were treated in ref. [3], and most active studies were carried

out at the kinetic level [3] which describes through the use of partial differential equations, the time evolution of the average but spatially resolved mice populations  $M_s$  (susceptible) and  $M_i$  (infected). The specific equations, with  $t$  denoting time and  $x$  representing location in a space of appropriate dimensions, a 2-d description being typically sufficient, are

$$\begin{aligned}\frac{\partial M_s}{\partial t} &= b(M_s + M_i) - cM_s - \frac{M_s(M_s + M_i)}{K(x, t)} - aM_sM_i + D\nabla^2 M_s, \\ \frac{\partial M_i}{\partial t} &= -cM_i - \frac{M_i(M_s + M_i)}{K(x, t)} + aM_sM_i + D\nabla^2 M_i.\end{aligned}\tag{1}$$

Considerations such as those arising from gender and age of the animals were tacitly neglected, and all parameters except  $K$  were considered to be independent of time.

The parameters of the model are  $a, b, c, K$  and  $D$ . All processes are assumed to be occurring continuously in time, an approximation which seems reasonable unless observations or phenomena are particularly chosen to be probed at very short time scales. The processes of birth and death of the mice are represented as occurring at rates  $b$  and  $c$ , respectively. The transmission of infection occurs through encounters, the aggression parameter being  $a$ . Saturation of the population is assumed to occur by competition for the resources among the mice through the environmental parameter  $K$  which describes nutrition available to the mice. This parameter, whose product with  $b - c$  is called the ‘carrying capacity’, controls the so-called logistic term which resolves in the standard manner the paradox of Malthusian explosion of the population.

Let us focus on this kinetic level model and refer to it as has been done in the current literature [11, 12] as the AK model. It may be regarded from the ecological viewpoint merely as the familiar SI model extended to include spatial resolution and diffusive transport. From the mathematical point of view it may be said to represent a system obeying the Fisher equation [10] with *internal states* representing infection or its absence, respectively. While near-trivial to conceive, this model has had considerable success in the short time since it was proposed for the Hantavirus [3]. It has led to qualitative and semi-quantitative success in explaining observations such as spatio-temporal patterns in the epidemics. These patterns are associated with correlations between periods of precipitation and epidemic outbreaks, and with the spatial location of refugia—regions of the landscape in which infection persists during off-periods of the epidemic [3, 5]. Other applications of the model include the detailed understanding and control of traveling waves of infection [4], fluctuations arising from the finiteness of the numbers and discreteness of the population of the rodents [11, 12], environmental effects [13], curious switching effects that have been predicted to occur [14], and extensions to unrelated systems such as bacteria in Petri dishes [15, 16].

The success of and interest in this so-called AK model represented by (1) led to recent attempts to devise practical prescriptions for the extraction of the parameters constituting the model from field measurements. The mouse birth rate  $b$  and the death rate  $c$  are obtained from field observations without too much trouble and are generally considered to be constants in space and time. With some effort, reasonable estimates of the environment resource parameter  $K(x, t)$  as a function of location and time can be obtained by counting food (such as nuts and water) available to the mice in the different locations, as well as by acquiring aerial photographs of the vegetation cover. Relative, rather than absolute, quantification of  $K$  is possible in this way. Observational collection of data concerning the aggression rate  $a$ , through which infection is thought to be transmitted during mouse-mouse encounters, turns out to be so difficult that, at least at the present moment, it must be considered an adjustable parameter. It was, however, possible to focus on the important parameter, the mouse diffusion constant  $D$ , and to obtain it quantitatively from field measurements [17, 18, 19].

The basic idea behind the extraction of  $D$  was to regard to the extent possible that the mouse movement is a simple random walk, and to extract  $D$  from records of the movement through the use of the well-known proportionality of the mean square displacement to  $Dt$ . The details of the theory [19] and the implementation of the prescriptions obtained from the theory to mark-recapture observations carried out in Panama [17] and New Mexico [18] may be found in our recent work. The important and perhaps surprising conclusion that emerged from that work was that the mouse mean square displacement, which grows linearly with  $t$  for short times, is found to *saturate* at large times. The appearance of a length scale in the random movements of the mice may be ascribed to the fact that animals typically move near fixed locations (burrows) for reasons of shelter and security [20, 21, 22], but it could also be ascribed to the fact that mark-recapture observations employ a limited region of space where the traps are laid out. It is possible to show analytically [17] that either of these factors could independently lead to the saturation of the mean square displacement. A disentangling of the two length scales was possible and led to explicit deductions of both the diffusion constant of the mice and their home ranges. Thus, reasonable realistic extracted values of the home range size  $L$  for different types of mice in different environments were found to be between 50 and 120 m for *Zygodontomys brevicauda* in Panama and about  $100 \pm 25$  m for *Peromyscus maniculatus* in New Mexico. The respective values of the diffusion constant  $D$  of the mice turned out to be  $200 \pm 50$  and  $470 \pm 50$  meters squared per day.

This quantitative information has provided the impetus (indeed, necessity) to generalize the AK model expressed in Eq. (1) to incorporate home ranges. Kenkre has suggested [23] several different generalizations for this purpose. One simple way of incorporating home ranges in our model of epidemic spread is to add potential terms to Eq. (1). Such an analysis, carried out by MacInnis et al. [24] has resulted in modifications in the AK predictions for refugia sizes and shapes. Another, simpler, model modification in the AK equations has led us [25] to apply the so-called Montroll defect technique [26] to deduce memory-possessing variations of the AK equations on the one hand and time-dependent diffusion constant variations on the other. Perhaps the most fertile model that has emerged from the work on the determination of motion and demographic characteristics is the one that we discuss in the present paper. It is set out in Sec. II below and an examination of its consequences form the rest of the paper.

## II. A GENERALIZED MODEL FOR THE SPREAD OF THE HANTAVIRUS

Let us consider the dynamics of two types of mice, stationary and itinerant (and susceptible and infected in each category). The stationary mice are the adults that move within their home ranges and do not stray far from the burrow. We have termed them ‘localized adults’ in the title of the present paper. For the sake of simplicity as well as to emphasize the new features that appear as a result of confinement, we neglect here the fact that home ranges may overlap and lead thereby to transmission of infection. The itinerant mice are the subadults (called ‘itinerant juveniles’ in the title) that must leave to find their own home ranges. Adults do not move because their home ranges are considered of negligible extent for the purposes of this description. They die at the rate  $c$  and have the standard logistic competition interactions with the environment controlled by the environment parameter  $K$ . They may be infected or not, the only possibility of their contracting infection being when an infected juvenile visits their home range. If infected, they may transmit infection to a susceptible juvenile if it visits their home range. Adults are not born but juveniles turn into adults. This happens when a juvenile finds an appropriate site to settle down in, which then becomes its burrow.

Juveniles are born at a rate  $b$  from the adult population. They are mobile, their motion being diffusive. They may acquire or transmit infection to other adults or other juveniles on encounter. If they find an appropriate site they turn into adults and become immobile as described above. They also have environment competition rates with the rest of the mice. In order to focus attention on special features of our generalization, we neglect the death rate  $c_B$  of the juveniles and allow their population to be depleted only through the competition term and their conversion to adults through growth. In a companion paper [27] we have included the death rate of the juveniles and indeed examined the specific effect of changes in that rate induced by the existence of predators in the open field.

The characteristics that we have described above suggest that the AK model in (1) be replaced by

$$\begin{aligned}
\frac{\partial B_i(x,t)}{\partial t} &= -c_B B_i - \frac{B_i(A+B)}{K(x,t)} + aB_s(A_i + B_i) + D\nabla^2 B_i - G(x)B_i, \\
\frac{\partial B_s(x,t)}{\partial t} &= bA - c_B B_s - \frac{B_s(A+B)}{K(x,t)} - aB_s(A_i + B_i) + D\nabla^2 B_s - G(x)B_s, \\
\frac{\partial A_i(x,t)}{\partial t} &= -cA_i - \frac{A_i(A+B)}{K(x,t)} + aA_s B_i + G(x)B_i, \\
\frac{\partial A_s(x,t)}{\partial t} &= -cA_s - \frac{A_s(A+B)}{K(x,t)} - aA_s B_i + G(x)B_s.
\end{aligned} \tag{2}$$

where  $A$  and  $B$  (without suffixes) denote the total densities of the adult and juvenile mice respectively, the suffixes  $i$  and  $s$  represent infected and susceptible states as earlier, and the last terms in each equation describe the settling down of the juveniles into their own homes, accompanied by their conversion into (static) adults. The rate of such conversion is  $G(x)$ . This  $G(x)$  is non-zero only if  $x$  lies in the ‘green pastures’, that is the spatial regions that the juveniles find suitable as their home ranges. Note that there are no spatial derivatives in the equations for the adults because the adults do not move, that being an extreme representation of their confinement to their home ranges.

The model represented in Eq. (2) describes the processes at a kinetic level as does the AK model in Eq. (1). This means that the key quantities are mice *densities* and that the evolution is described via *kinetic* equations such as the Fisher equation [9, 10]. A less detailed description, with no spatial resolution included, is provided by a mean field model in which the key quantities are the total mice numbers  $\int A(x,t)dx$  and  $\int B(x,t)dx$  where the integrals are over the entire landscape. A *more* detailed description than in kinetic models is provided by configuration master equation approaches (see for example [28, 29]) which include fluctuation effects. In the present paper we will analyze both the mean field and the configuration master equation approaches, reserving the middle-level kinetic treatment for a future publication.

Our paper is laid out as follows. In Sec. III, we present an explicit analysis of the mean field model, and the simulation treatment of the configuration level approach. In Sec. IV, we present essential results and their discussion. In Sec. V, we present concluding remarks.

### III. ANALYSIS: MEAN FIELD AND SIMULATION TREATMENTS

In this section we treat the model of Eq. (2) first by simplifying it to the mean field level of description and then by augmenting it to the configuration level description. For simplicity we keep  $K$  time and space independent.

#### A. Mean field Description

The mean field description focuses on the time evolution of the integrals of the densities in a kinetic description such as that of Eq. (2) and thereby loses space resolution. Called in some contexts the ‘well-stirred limit’, the mean field description may be considered as the limit of Eq. (2) for an infinitely large diffusion constant  $D$ . In passing from the kinetic to the mean field description, the single infection quantity  $a$  in Eq. (2) results in *two* corresponding quantities:  $a_0$  and  $a_1$ . The former (latter) refers to the transfer of infection between an adult (juvenile) and a juvenile. Both quantities result from the combination of the infection event and the motion process. The latter is explicit in Eq. (2) but not in Eq. (3). The difference between  $a_0$  and  $a_1$  is precisely the difference between the expression  $4\pi RD$  and  $8\pi RD$  which describes the capture and mutual annihilation rates respectively in the literature on excitons in molecular crystals [30, 31]. Although the precise relationship of  $a_0$  and  $a_1$  would depend on the relative importance of the mice motion and infection processes, we will take  $a_1 = 2a_0$  for simplicity in the rest of the paper in keeping with the extreme limits considered in other literature contexts [32].

The juveniles transmit infection among themselves with rate per unit density  $a_1$ , get infected and transmit infection to the adults with rate per unit density  $a_0$ , struggle for resources all over space through the environment parameter  $K$  and become adult with a growth rate  $g$ . This growth rate, introduced to represent a juvenile settling into an unoccupied home range and growing into an adult, is proportional to  $G(x)$  of Eq. (2). The other terms can be interpreted as explained above for Eq. (2). The coupled set of equations for normalized quantities in the mean field description is

$$\begin{aligned}\frac{d\mathcal{B}_i}{d\tau} &= -\gamma\mathcal{B}_i + \alpha_0\mathcal{B}_s\mathcal{A}_i + \alpha_1\mathcal{B}_i\mathcal{B}_s - \mathcal{B}_i(\mathcal{A} + \mathcal{B}), \\ \frac{d\mathcal{B}_s}{d\tau} &= -\gamma\mathcal{B}_s + \beta(\mathcal{A}_s + \mathcal{A}_i) - \alpha_0\mathcal{B}_s\mathcal{A}_i - \alpha_1\mathcal{B}_i\mathcal{B}_s - \mathcal{B}_s(\mathcal{A} + \mathcal{B}), \\ \frac{d\mathcal{A}_i}{d\tau} &= -\mathcal{A}_i + \alpha_0\mathcal{A}_s\mathcal{B}_i + \gamma\mathcal{B}_i - \mathcal{A}_i(\mathcal{A} + \mathcal{B}), \\ \frac{d\mathcal{A}_s}{d\tau} &= -\mathcal{A}_s - \alpha_0\mathcal{A}_s\mathcal{B}_i + \gamma\mathcal{B}_s - \mathcal{A}_s(\mathcal{A} + \mathcal{B}).\end{aligned}\tag{3}$$

where each script character denotes the ratio of the quantity described by the corresponding Roman character and  $cK$ . Thus,  $\mathcal{A}_i = A_i/(cK)$ . We also write  $\tau = ct$  and the dimensionless parameters are now  $\gamma = g/c$ ,  $\beta = b/c$ ,  $\alpha_0 = Ka_0$ , and  $\alpha_1 = Ka_1$ . As explained above we take  $a_1 = 2a_0$ .

From Eq. (3) it is easy to recognize that the total adult and juvenile populations, respectively,  $\mathcal{A} = \mathcal{A}_i + \mathcal{A}_s$  and  $\mathcal{B} = \mathcal{B}_i + \mathcal{B}_s$ , obey the following evolution

$$\begin{aligned}\frac{d\mathcal{B}}{d\tau} &= \beta\mathcal{A} - \gamma\mathcal{B} - \mathcal{B}(\mathcal{A} + \mathcal{B}), \\ \frac{d\mathcal{A}}{d\tau} &= -\mathcal{A} + \gamma\mathcal{B} - \mathcal{A}(\mathcal{A} + \mathcal{B}).\end{aligned}\tag{4}$$

Even if  $\mathcal{A}$  and  $\mathcal{B}$  are both limited by a quadratic saturation, it is evident from (4) that the sum  $\mathcal{A} + \mathcal{B}$  does not obey the standard logistic equation. This fact, as we will see in Sec. IV, gives some qualitative differences of the steady state parameters dependence of (3) from the AK model. The steady state values  $\overline{\mathcal{A}}$  and  $\overline{\mathcal{B}}$  are given for  $\beta > 1$  by

$$\begin{aligned}\overline{\mathcal{A}} &= \gamma \frac{1 + \xi - \sqrt{1 + 2\xi}}{\xi}, \\ \overline{\mathcal{B}} &= \frac{1 + \xi - \sqrt{1 + 2\xi}}{\xi} \left[ 1 + \frac{(\gamma + 1)}{2} (\sqrt{1 + 2\xi} - 1) \right],\end{aligned}\tag{5}$$

with  $\xi = 2(\beta - 1)\gamma/(1 + \gamma)^2$ . The situation  $\beta > 1$  represents the juvenile birth rate  $b$  being larger than the adult death rate  $c$ . For the opposite situation,  $\beta < 1$ , when the adults die quicker than the juveniles are born, the trivial solution  $\bar{\mathcal{A}} = \bar{\mathcal{B}} = 0$  emerges from Eq. (4). These two steady states exchange their stability as  $\beta$  crosses the value 1 clearly indicating the presence of a transcritical bifurcation at  $\beta = 1$  from zero to non zero population density.

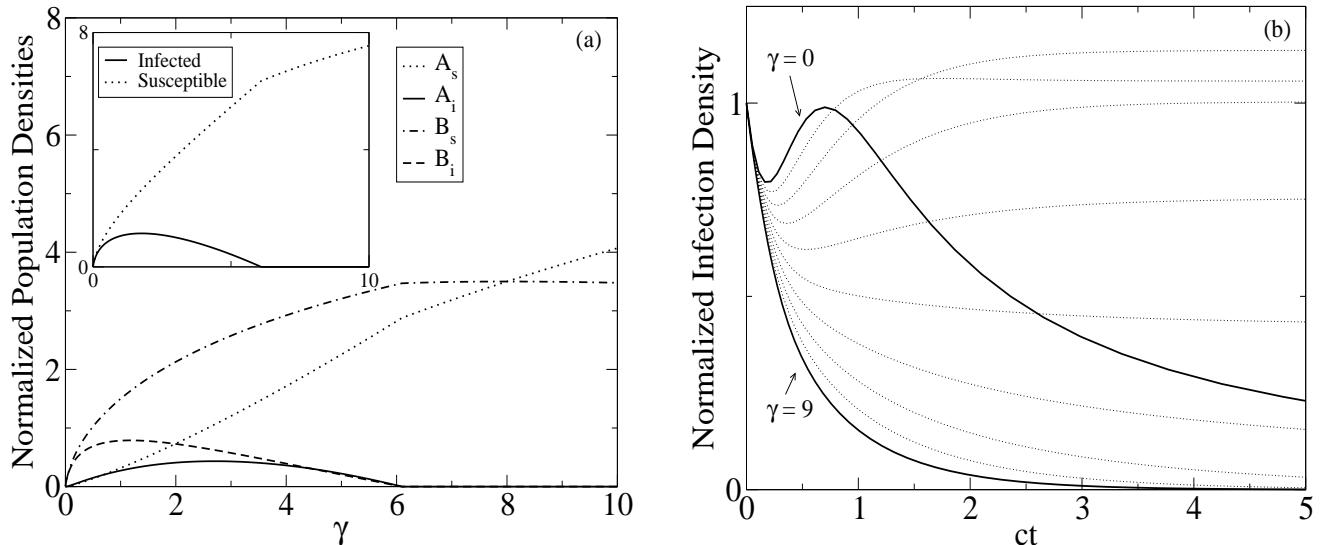


FIG. 1: Effect of variation in the growth rate on mice densities as given by the mean field description. Steady state mice densities are plotted in (a) against the normalized growth rate  $\gamma$  ( $= g/c$ ) at which juveniles grow into adults, and the evolution of the total density of infected mice, normalized to its initial value, is plotted in (b) against the normalized time  $ct$ . Both exhibit non-monotonic behavior, for instance, a rise in infection as  $\gamma$  is increased from zero and a decay beyond a certain value. System parameters have been chosen to be  $\alpha_0 = 1.1$  and  $\beta = 15$ . In (a), the four mice densities have been shown in the main figure and the total infected and susceptible densities, sums of adult and juvenile contributions, are shown in the inset with axes identical to the main figure. In (b), the ten curves are for  $\gamma$  incremented by 1 from 0 to 9 and go down the graph in order for short times but for long times approach equilibrium values that are not in the same order. Notice also the peculiar non-monotonicity in time.

With the help of the non-zero steady state values  $\bar{\mathcal{A}}$  and  $\bar{\mathcal{B}}$  in Eq. (4) it is possible to obtain (see Appendix) the steady state solutions of Eq. (3). The system has the trivial solution ( $\bar{\mathcal{A}}_i = \bar{\mathcal{A}}_s = \bar{\mathcal{B}}_i = \bar{\mathcal{B}}_s = 0$ ) when  $\beta < 1$ , and two possible steady states for  $\beta > 1$ . They represent respectively the non-infected and infected phase. The former is given by

$$\begin{aligned}\bar{\mathcal{B}}_i &= 0, \\ \bar{\mathcal{B}}_s &= \bar{\mathcal{B}}, \\ \bar{\mathcal{A}}_i &= 0, \\ \bar{\mathcal{A}}_s &= \bar{\mathcal{A}},\end{aligned}\tag{6}$$

while the latter is given by

$$\begin{aligned}\bar{\mathcal{B}}_i &= \frac{\sqrt{\mathcal{F}^2 + 8\mathcal{E}} - \mathcal{F}}{4\alpha_0}, \\ \bar{\mathcal{B}}_s &= \bar{\mathcal{B}} - \bar{\mathcal{B}}_i, \\ \bar{\mathcal{A}}_i &= \frac{\bar{\mathcal{B}}_i (\gamma + \alpha_0 \bar{\mathcal{A}})}{\alpha_0 \bar{\mathcal{B}}_i + 1 + \bar{\mathcal{A}} + \bar{\mathcal{B}}}, \\ \bar{\mathcal{A}}_s &= \bar{\mathcal{A}} - \bar{\mathcal{A}}_i,\end{aligned}\tag{7}$$

wherein  $\mathcal{F} = 2(\gamma + 1) + \bar{\mathcal{A}}(3 + \alpha_0) + \bar{\mathcal{B}}(3 - 2\alpha_0)$  and  $\mathcal{E} = \alpha_0 \bar{\mathcal{B}} (\gamma + \alpha_0 \bar{\mathcal{A}}) - [\gamma + \bar{\mathcal{A}} + \bar{\mathcal{B}}(1 - 2\alpha_0)] (1 + \bar{\mathcal{A}} + \bar{\mathcal{B}})$ . A stability analysis (see Appendix) shows that the solution sets represented by Eqs. (6) and (7) exchange their stability through a transcritical bifurcation when the normalized infection rate is larger than a critical value  $\alpha_c$ . By determining

when  $\mathcal{E} = 0$  we can calculate the critical value as shown in the Appendix. Equivalently, by studying the non-normalized mean field equations, we can calculate the critical environment parameter  $K_c$ :

$$K_c = \frac{\gamma + 2(1 + \bar{A} + \bar{B})}{2a_0\bar{A}} \left\{ \sqrt{1 + \frac{4\bar{A}(\gamma + \bar{A} + \bar{B})(1 + \bar{A} + \bar{B})}{\bar{B}[\gamma + 2(1 + \bar{A} + \bar{B})]^2}} - 1 \right\}. \quad (8)$$

Here  $\bar{A} + \bar{B}$  is the total population at steady state, i.e., the carrying capacity of the system normalized to  $cK$ :

$$\bar{A} + \bar{B} = (\beta - 1) \frac{\gamma}{1 + \gamma} \frac{\sqrt{1 + 2\xi} - 1}{\xi}. \quad (9)$$

An infected phase exists for  $K > K_c$ .

## B. Simulation Description

It is well-known [33] that spatial aspects, not accessible to mean field theory, are (obviously) very important in epidemiology, generally in ecology, and that they require a description, capable of addressing spatial correlations. One way to treat spatial resolution is to adopt kinetic level approaches as in the AK model, while another, a more detailed way, is to adopt an approach based on the evolution of the full configuration states. We have elected to choose the latter in the present paper. Analytic solutions are typically impossible in such an approach except for oversimplified models. Hence we resort to simulations as done previously [11] for the AK model.

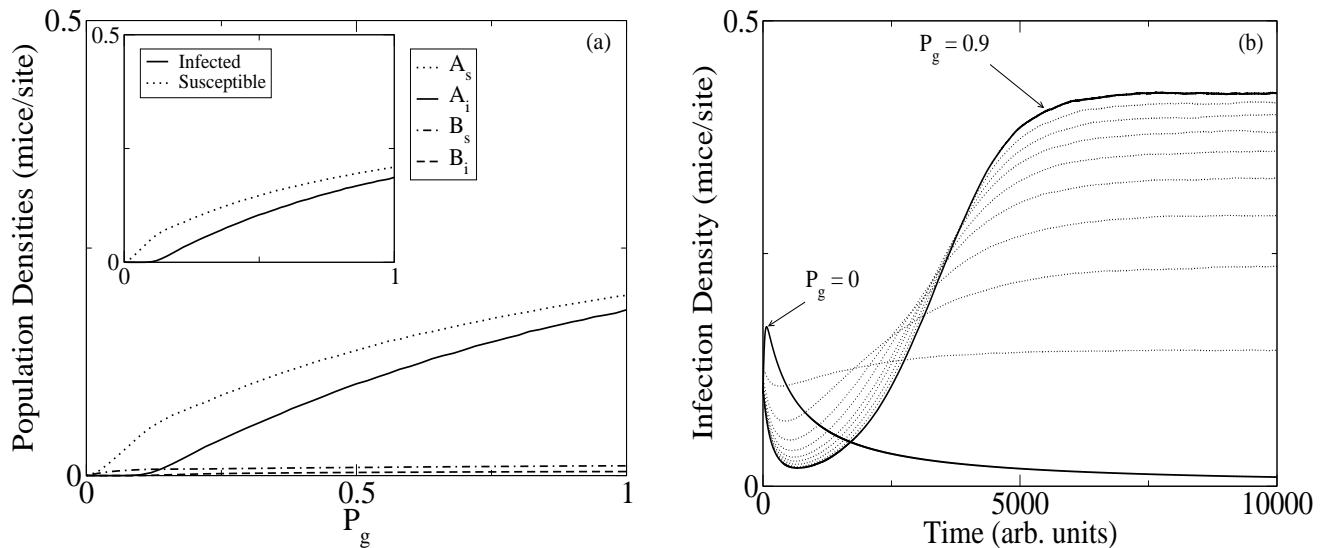


FIG. 2: Effect of variation in the growth probability as given by the simulation description. Compare with Fig. 1. Steady state mice densities are plotted in (a) against  $P_g$  and the time evolution is shown in (b) where the ten curves correspond to increments of 0.1 in  $P_g$ . Contrary to the mean-field model (see Fig. 1), where infected population as function of the growth rate  $\gamma$  always displays a non-monotonic behavior, here the infected population has a monotonic increase with  $P_g$ . The parameters for both (a) and (b) are  $P_c = 0.01$ ,  $P_b = 0.011$ ,  $P_a = 0.3$  and  $P_K = 0.99$ .

Our simulations are carried out on a  $L \times L$  square lattice with each site of the lattice corresponding to a small region in the landscape. Moderately large lattices (with a total of  $2^{14}$  sites) have been used in the simulations. The four subclasses of mice, (adults and juveniles in susceptible and infected states) change their numbers, as time evolves, in accordance with rules which represent the model under consideration. At each time step, the juveniles may move but the adults not, the probability for the diffusive (random walk) motion being 0.125 for any of the eight directions of the square lattice. We consider the time step scaled to the diffusion constant in this manner. An adult, infected or susceptible, gives birth to a susceptible juvenile with probability  $P_b$ . An adult dies by aging with probability  $P_c$ . If two or more mice meet at a site, one of them may die with probability  $1 - P_K$ . If a susceptible mouse occupies the same site as an infected mouse, the former has probability  $P_a$  of getting infected in the next time step. And if a

juvenile mouse finds itself at a site without an adult, it grows up and settles at that site with probability  $P_g$ . These rules represent a simplified version of Eq. (2) augmented to the configuration level. It is simplified in that the regions ('green pastures') where the juveniles may settle down have not been marked but the process has been represented through a probability of conversion. We have carried out full scale simulations which take into account the spatial extent of the green pasture regions and will discuss the results elsewhere.

The simulation description thus has the parameters,  $P_b$ ,  $P_c$ ,  $P_g$ ,  $P_a$ , and  $P_K$ , in correspondence to the respective rates  $b$ ,  $c$ ,  $g$ ,  $a_0$ , and  $K$  of the mean field equations analyzed above. However, the correspondence is not straightforward in all cases, as expected. Extensive computer simulations were performed. We found that the system reaches a steady state, after a transient. The main quantities we analyzed were the densities of the four populations of mice and the existence or not of infection in the steady-state. Densities are defined as the total number of mice in the lattice divided by the total volume (or area) of the lattice. Since the existence of more than one adult per site is not allowed, the density of adults lies between 0 and 1. By contrast, the juvenile density may exceed 1.

#### IV. RESULTS

The main difference between the mean field and the simulation results lies in the effects of the quantities that govern the growth of juveniles into adults, rate  $g$  and probability  $P_g$ , respectively. We show this dependence respectively in Figs. 1 and 2. From Fig. 1(a) we see a non-monotonic dependence of the steady state infected population densities as  $\gamma$  increases. This non-monotonicity is also evident in Fig. 1(b) where the time evolution for the entire infected population is shown for different values of  $\gamma$ . In the limit  $\gamma \rightarrow 0$  in Eq. (5)  $\overline{A}, \overline{B} \rightarrow 0$  since no new adult can be 'born' (i.e., produced by conversion of a juvenile through growth), the juvenile population cannot be regenerated and dies out because of competition, and eventually no population can be sustained. The juveniles are responsible for spreading the infection to the adults and a larger number of them tends to increase the infected population. However if the juveniles convert into adults too fast, there are less mobile carriers of infection, the number of infected juveniles decreases (note that juveniles are born susceptible and never infected, this being a Hantavirus characteristic), and eventually the infection disappears. In other words we can say that as  $\gamma$  grows, the critical environment parameter  $K_c$  eventually becomes smaller than the system  $K$ .

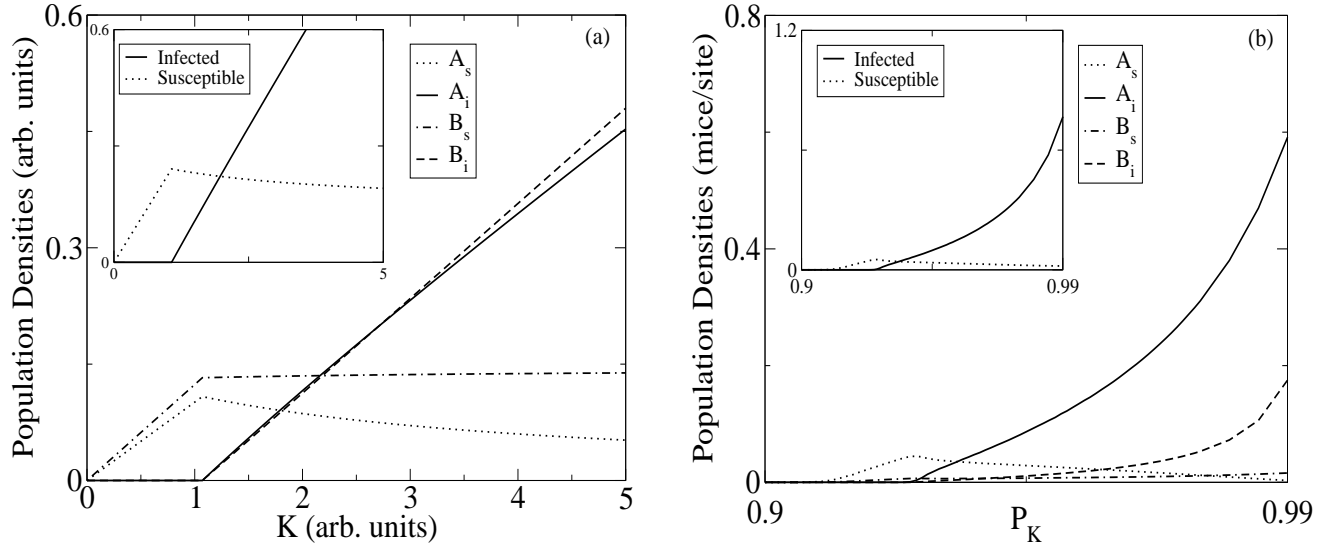


FIG. 3: Steady state densities versus the environment parameter plotted from the mean field description in (a) and the simulation description in (b). The x-axis coordinate in the inset and the main figure is  $K$  in (a) and  $P_K$  in (b). Other parameters are taken to be  $\beta = 1.5$ ,  $\gamma = 1$  and  $a_0 = 1$  in arbitrary units in (a) and  $P_c = 0.01$ ,  $P_b = 0.014$ ,  $P_g = 0.1$  and  $P_a = 0.3$  in (b). The behavior is similar in both levels of description. When the environment parameter is large enough, an infected phase emerges. Once that happens, the increase of the population is due only to a larger density of infected animals, the susceptible population decreasing its overall density to a constant. The susceptible population in the simulation description becomes zero for  $P_K$  smaller than a critical value that depends primarily on the value of  $P_b$  relative to  $P_c$ . If  $P_b$  is sufficiently close to  $P_c$ , as is the case shown here, competition and adult death processes drive the entire system to extinction at a nonzero value of  $P_K$ .

In Fig. 2(a) we show the  $P_g$  dependence of the steady state populations in the simulation description. This is a noteworthy difference from Fig. 1(a): a monotonic increase of the infected population. This difference has to be ascribed to a spatial correlation effect. Since there can be only one adult per site, an increase in  $P_g$  has also the effect of reducing the number of available sites for the juveniles. For sufficiently large values of  $P_g$ , clusters of adults start to form, creating confined regions in the landscape where the juveniles are constrained to roam. This in turn increases dramatically the average time necessary for a juvenile to find an available site to settle down. Unfavorable effects of the growth of juveniles into adults observed in the mean field theory do not therefore occur in the simulations as a result of the spatial correlations set up by the cluster formation in the adults. The monotonic increase of the infected population as function of  $P_g$  can also be observed in Fig. 2(b) where the time evolution for different  $P_g$  values is depicted. In order to verify the validity of the above explanation of the difference in the mean field and simulation predictions, we studied a *pseudo-model*, intermediate between the two descriptions. In the pseudo-model, a juvenile can move to an arbitrary position and not only to a nearest-neighbor site, thus being able to jump the barriers set up by the clusters formed in the adult population. Careful simulations we have carried out show that, indeed, the steady state populations have an infected phase that decays to zero beyond a critical value of  $P_g$ : the pseudo-model predicts the same qualitative behavior as the mean field theory.

The struggle for resources described at the mean field level by the environment parameter  $K$  is here represented by the probability of survival  $P_K$ : the probability of dying via competition for resources is  $1 - P_K$ . In Fig. 3(a) we show the steady state populations as function of  $K$  in the mean field description and in Fig. 3(b) the corresponding results as function of  $P_K$  in the simulation description. The behaviour in the two cases is similar: beyond the critical value of  $K$  ( $P_K$ ) the infected population increases with a sublinear dependence on  $K$  ( $P_K$ ).

## V. CONCLUDING REMARKS

From a perspective of concepts that have been successful in physics, our present model of the mice assembly may be described by the term *liquid-solid* because it describes a class of mice that move freely as do the molecules of a liquid, and another class of mice that move in the neighborhood of fixed positions (the burrows) as do the molecules of a solid, which vibrate around fixed lattice sites. Therefore, for the purposes of the following discussion, we will call our model the liquid-solid (LS) model.

Although the LS model was constructed by generalizing the structure of the AK model, the two have really only one parameter truly in common: the environment parameter  $K$ . The birth rate  $b$  in the AK model describes the emergence of new mice from all mice whereas it produces only juveniles from adults in the LS model. The death rate  $c$  in the AK model is similarly applicable to all mice but in the present version of the LS model it applies only to the adults. In addition to depletion via competition for resources, the disappearance of the juveniles is assumed to occur only through the growth rate  $g$  when they grow up into adults. The diffusion constant  $D$  describes the motion of all mice in the AK model but only of the juveniles in the LS model, the adults being stationary. Therefore, we make comparison comments regarding the two models by looking at how the infection depends on  $K$ . For simplicity we discuss this comparison at the mean field level.

At first sight, it might appear that the LS model does not reduce to the AK counterpart in any situation. However there exists one such limit. Let  $K$  be infinite so that the carrying capacity is infinite also. To eliminate runaway solutions in the steady state, let us take the birth and death rates equal in the AK model so that  $b_{AK} = c_{AK}$ , and let us correspondingly take the birth-death ratio  $\beta = 1$  in the LS model. Consider now the limit in which the growth rate  $g$  of the juveniles and the death rate  $c$  of the adults in the LS model are much larger than the rate of infection between adults and juveniles but such that  $\gamma = g/c$  is finite. In such a situation the adults constitute an isolated reservoir of the infection: they do not play any role in spreading it since an adult is infected only if it ‘grew up’ from an infected juvenile. In particular, it can be shown that by considering  $a_1 = a_{AK}$  and  $\gamma = \left[ (1 + 4c_{AK})^{1/2} + 1 \right] / 2$ , where  $a_{AK}$  is the infection parameter in the AK model, our present model at steady state gives *exactly* the same analytic dependence of the AK model for the infected and susceptible population as function of  $c_{AK}$  and  $a_{AK}$ .

This equivalence suggests a simple way to compare the two models, when  $K$  is finite, by considering that no transmission of infection occurs between adults and juveniles, i.e.,  $a_0$  is taken to be zero in the LS model. In such a scenario, the two models have the same qualitative dependence of the infected and susceptible populations as function of the environment parameter: for  $K > K_c$  the susceptible population remains constant while the infected population increases linearly. In other words, by increasing  $K$ , the additional population (proportional to  $K$ ) that the environment can sustain eventually becomes infected at steady state. In Fig. 4 we show this dependence for the AK model at the mean field (Fig. 4(a)) and at the simulation description (Fig. 4(b)), respectively. The behavior is similar in both levels of description. When the environment parameter is large enough, an infected phase emerges. Once that happens, the increase of the population is due only to a larger density of infected animals, the susceptible



population remaining constant. By contrast, as previously shown in Fig. 3, the infected populations increase while the susceptible populations decrease to a non zero value as  $K > K_c$ . At the mean field description it is also evident that the infected population increases only sub-linearly as function of  $K$  and not linearly as in the AK model.

We indicate how our theoretical predictions may be used in conjunction with observations in the field to test the validity/applicability of the LS model. The qualitative differences between the AK and LS models discussed above could be exploited in analyzing data from *mark-recapture* observations. In such observations, traps are set up in regions in the landscape and mice are caught, examined, marked, and released. Information about a variety of features is gathered including infection status and age. Juveniles have clear physiological characteristics that distinguish them from the adults [21]. If all other effects are controlled, supplementing additional food homogeneously over the terrain would be a way to increase the environment parameter  $K$ . Experiments that exploit this feature may allow one to determine if, in the presence of infection, the susceptible population remains constant or decreases as the amount of food is increased. This would allow us to establish whether the juveniles are indeed the main carrier of the disease and whether augmenting the AK considerations to the LS model is the correct way of analyzing the spread of the Hantavirus infection.

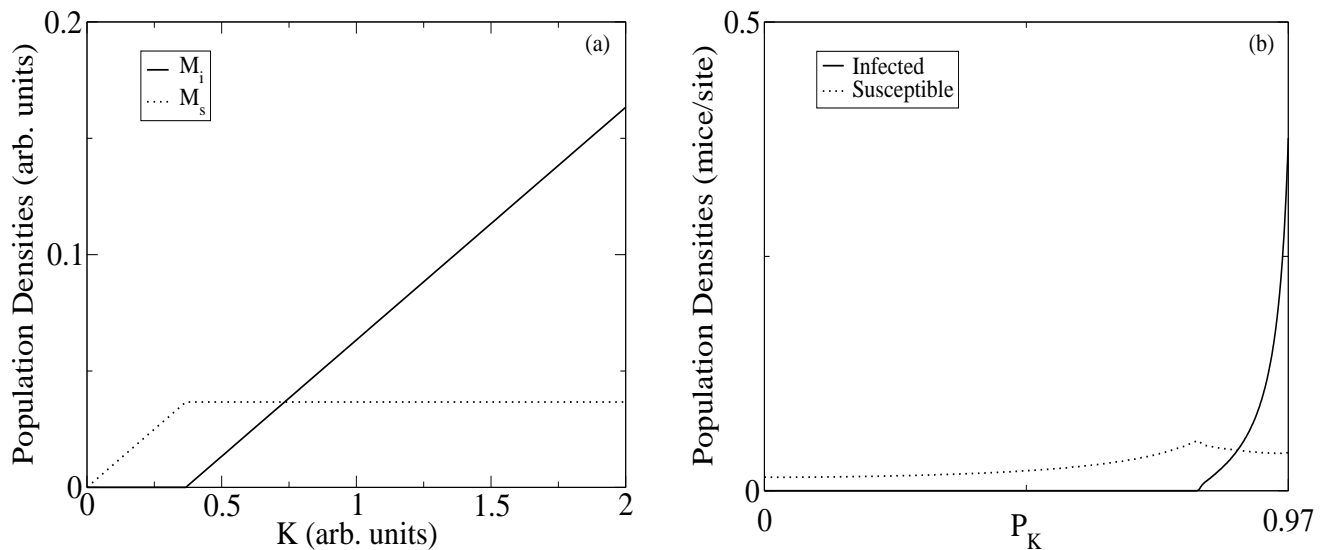


FIG. 4: Steady state densities of the Ak model as function of the environment parameter plotted from the mean field description in (a) and the simulation description in (b). The x-axis is the environment parameter  $K$  in (a) and the probability  $P_K$  in (b). Other parameters are taken to be  $\beta = 1.1$ , and  $a_{AK} = 30$  in arbitrary units in (a) and  $P_c = 0.01$ ,  $P_b = 0.02$ , and  $P_a = 0.6$  in (b).

Since in both models the value of  $K_c$  depends on all the other parameters, there are obviously situations in which one model predicts infection while the other does not. However, if we compare the amount of infection as  $K$  increases beyond  $K_c$ , our analysis shows that the AK model gives more infection than the LS model. Surely, this is to be expected since, in the latter, part of the population (adults) is stationary and transmit infection less efficiently. This is an important consequence of the existence of home ranges determined quantitatively in our recent work [17, 18, 19]. Our analysis allows us to quantify that consequence, i.e. to determine how much the reduced motion of the adults decreases the transmission of infection compared to the AK model. While, for simplicity, we have considered here the extreme limit of zero overlap between neighboring home ranges, to what extent the degree of home range overlap will change our conclusions is an open problem and the subject of our current investigations.

To keep our analysis focussed on essentials, we have considered in the present paper the case in which the juvenile population is depleted only through growth into adults and not through death. We have carried out mean field as well as spatially resolved studies of the situation when this simplification does not apply. This is important because, in their itinerant attempts to find suitable places for their own home ranges, juveniles are surely exposed to predators that kill them. Details of the investigation will be given elsewhere [27] but we report here that we have uncovered the epidemiologically noteworthy possibility of buffering the transmission of the infection by introducing predators in the landscape. Sustained by a sufficiently large  $K$  (environment resources), a large *susceptible* population of mice can exist but with no infection as a consequence of interaction with predators.

Among additional avenues of theoretical research based on the LS model are the study of spatial correlations based

on modern techniques [34], the extension of our analysis by specifying the spatial dependence of rates  $G(x)$  in Eq. (2) so that the effects of the location of the ‘green pastures’ can be ascertained, and the comparison of our predictions to observations in the field concerning infection spread. The latter effort is particularly important because it will allow us to explore the applicability and practical relevance of home range inclusion in the theory of the spread of the Hantavirus. Research in all these directions is under way.

### Acknowledgments

We acknowledge valuable conversations with Bob Parmenter and Terry Yates about the Hantavirus epidemic and with Marcelo Kuperman about aspects of its description. This work was supported in part by the NSF under grant no. INT-0336343, by NSF/NIH Ecology of Infectious Diseases under grant no. EF-0326757, by CONICET (PEI 6482), by ANPCyT (PICT-R 2002-87/2), and by DARPA under grant no. DARPA-N00014-03-1-0900. We acknowledge the Center for High Performance Computing, UNM, for making available to us their computing resources.

### VI. APPENDIX

Since the total adult and juvenile population in (5) is known in terms of the parameters  $\xi$  and  $\gamma$ , the set of equations (3) at steady state can be simplified considerably to

$$\begin{aligned}\alpha_0 \bar{\mathcal{B}}_s \bar{\mathcal{A}}_i + \alpha_1 \bar{\mathcal{B}}_s \bar{\mathcal{B}}_i - \bar{\mathcal{B}}_i (\gamma + \bar{\mathcal{A}} + \bar{\mathcal{B}}) &= 0, \\ \bar{\mathcal{B}}_i + \bar{\mathcal{B}}_s &= \bar{\mathcal{B}}, \\ (\gamma + \alpha_0 \bar{\mathcal{A}}_s) \bar{\mathcal{B}}_i - \bar{\mathcal{A}}_i (1 + \bar{\mathcal{A}} + \bar{\mathcal{B}}) &= 0, \\ \bar{\mathcal{A}}_i + \bar{\mathcal{A}}_s &= \bar{\mathcal{A}}.\end{aligned}\tag{10}$$

The system (10) has only three possible solutions with the four variables larger or equal to zero. The trivial one implies  $\bar{\mathcal{A}} = \bar{\mathcal{B}} = 0$ . The other two solutions can be obtained by reducing through substitution Eq. (10) to the following polynomial equation in  $\bar{\mathcal{B}}_i$

$$\begin{aligned}\bar{\mathcal{B}}_i \left\{ \alpha_0 \alpha_1 \bar{\mathcal{B}}_i^2 + \bar{\mathcal{B}}_i \left\{ \bar{\mathcal{A}} (\alpha_0^2 + \alpha_0 + \alpha_1) + \bar{\mathcal{B}} [\alpha_0 + \alpha_1 (1 - \alpha_0)] + 2\gamma \alpha_0 + \alpha_1 \right\} \right. \\ \left. + [\gamma + \bar{\mathcal{A}} + \bar{\mathcal{B}} (1 - \alpha_1)] (1 + \bar{\mathcal{A}} + \bar{\mathcal{B}}) - \alpha_0 \bar{\mathcal{B}} (\gamma + \alpha_0 \bar{\mathcal{A}}) \right\} = 0,\end{aligned}\tag{11}$$

from which it is easy to obtain the solutions shown in Eq. (6) and (7). The study of the sign of Eq. (11) gives the condition for the existence of an infected phase

$$\alpha_c = \frac{\gamma + 2(1 + \bar{\mathcal{A}} + \bar{\mathcal{B}})}{2\bar{\mathcal{A}}} \left\{ \sqrt{1 + \frac{4\bar{\mathcal{A}}(\gamma + \bar{\mathcal{A}} + \bar{\mathcal{B}})(1 + \bar{\mathcal{A}} + \bar{\mathcal{B}})}{\bar{\mathcal{B}}[\gamma + 2(1 + \bar{\mathcal{A}} + \bar{\mathcal{B}})]^2}} - 1 \right\},\tag{12}$$

which can be converted to a  $K_c$  as written in Eq. (8). Notice that the third root of the polynomial in (11) can be shown through a numerical study to be always negative and it is thus discarded.

The stability analysis of the three solutions of (3) is done by calculating the Jacobian of the system at steady state  $J(\bar{\mathcal{A}}_i, \bar{\mathcal{A}}_s, \bar{\mathcal{B}}_i, \bar{\mathcal{B}}_s)$

$$J = \begin{pmatrix} -(1 + \bar{\mathcal{A}} + \bar{\mathcal{B}} + \bar{\mathcal{A}}_i) & \alpha_0 \bar{\mathcal{B}}_i - \bar{\mathcal{A}}_i & & \\ -\bar{\mathcal{A}}_s & -(1 + \bar{\mathcal{A}} + \bar{\mathcal{B}} + \bar{\mathcal{A}}_s + \alpha_0 \bar{\mathcal{B}}_i) & & \\ \alpha_0 \bar{\mathcal{B}}_s - \bar{\mathcal{B}}_i & -\bar{\mathcal{B}}_i & & \\ \beta - (\alpha_0 + 1) \bar{\mathcal{B}}_s & \beta - \bar{\mathcal{B}}_s & & \\ \alpha_0 \bar{\mathcal{A}}_s - \bar{\mathcal{A}}_i & & -\bar{\mathcal{A}}_i & \\ -(\alpha_0 + 1) \bar{\mathcal{A}}_s & & \gamma - \bar{\mathcal{A}}_s & \\ 2\alpha_0 \bar{\mathcal{B}}_s - (\gamma + \bar{\mathcal{A}} + \bar{\mathcal{B}} + \bar{\mathcal{B}}_i) & & \alpha_0 \bar{\mathcal{A}}_i + (2\alpha_0 - 1) \bar{\mathcal{B}}_i & \\ -(\alpha_0 + 1) \bar{\mathcal{B}}_s & & -[\gamma + \bar{\mathcal{A}} + \bar{\mathcal{B}} + \bar{\mathcal{B}}_s + \alpha_0 (\bar{\mathcal{A}}_i + 2\bar{\mathcal{B}}_i)] & \end{pmatrix}\tag{13}$$

The trivial solution has the following four eigenvalues

$$\begin{aligned}\lambda_1 &= -1, \\ \lambda_2 &= -\gamma, \\ \lambda_3 &= -\frac{\gamma+1}{2} \left( \sqrt{1+2\xi} + 1 \right), \\ \lambda_4 &= \frac{\gamma+1}{2} \left( \sqrt{1+2\xi} - 1 \right),\end{aligned}\tag{14}$$

from which it is evident that  $\lambda_4 < 0$  if  $\beta < 1$ , while all the other eigenvalues are always negative. The trivial solution is thus stable if  $\beta < 1$  and it becomes unstable when  $\beta > 1$ .

The polynomial characteristic  $P(\lambda)$  of the Jacobian (13) associated with the solution (6) is equal to the product  $P_1(\lambda)P_2(\lambda)$  where

$$\begin{aligned}P_1(\lambda) &= \lambda^2 + \lambda [1 + 3(\bar{\mathcal{A}} + \bar{\mathcal{B}}) + \gamma] \\ &\quad + (1 + 2\bar{\mathcal{A}} + \bar{\mathcal{B}})(\bar{\mathcal{A}} + 2\bar{\mathcal{B}} + \gamma) - (\bar{\mathcal{B}} - \beta)(\bar{\mathcal{A}} - \gamma),\end{aligned}\tag{15}$$

and

$$\begin{aligned}P_2(\lambda) &= \lambda^2 + \lambda [1 + 2(\bar{\mathcal{A}} + \bar{\mathcal{B}}) - 2\alpha_0\bar{\mathcal{B}} + \gamma] \\ &\quad + (1 + \bar{\mathcal{A}} + \bar{\mathcal{B}})(\bar{\mathcal{A}} + \bar{\mathcal{B}} - 2\alpha_0\bar{\mathcal{B}} + \gamma) - \alpha_0^2\bar{\mathcal{A}}\bar{\mathcal{B}}.\end{aligned}\tag{16}$$

The eigenvalues associated to  $P_1(\lambda)$  are given by

$$\lambda_{1\pm} = \frac{1+\gamma}{4} \left[ 1 - 3\sqrt{1+2\xi} \pm \sqrt{2(1+\xi + \sqrt{1+2\xi})} \right],\tag{17}$$

with  $\lambda_{1-} < 0$  for any  $\beta$  and  $\gamma$  and  $\lambda_{1+} > 0$  when  $\beta < 1$ . The eigenvalues associated to  $P_2(\lambda)$  are negative for  $\alpha_0 < \alpha_c$  and they become positive when  $\alpha_0 > \alpha_c$ . The solution defined in Eq. (6) is thus unstable if either  $\beta < 1$  or if  $\alpha_0 > \alpha_c$ .

The study of the sign of the eigenvalues associated with the third possible steady state is done numerically and it is possible to show that Eq. (7) represents a stable steady state if  $\beta > 1$  and  $\alpha_0 > \alpha_c$  and become unstable if either  $\beta < 1$  or  $\alpha_0 < \alpha_c$ . The mean field description from the dynamical point of view has thus two transcritical bifurcations: one when the growth rate  $b$  equals the death rate  $c$  and the other one when the infection rate  $\alpha_0$  equals the critical infection rate  $\alpha_c$  or similarly when the environment parameter  $K$  equals the critical environment parameter  $K_c$ .

- 
- [1] T.L. Yates, J.N. Mills, C.A. Parmenter, T.G. Ksiazek, R.R. Parmenter, J.R. Vande Castle, C.H. Calisher, S.T. Nichol, K.D. Abbott, J.C. Young, M.L. Morrison, B.J. Beaty, J.L. Dunnun, R.J. Baker, J. Salazar-Bravo, C.J. Peters, *Bioscience* **52**, 989 (2002).
- [2] J.N. Mills, T.L. Yates, T.G. Ksiazek, C.J. Peters, J.E. Childs, *Emerging Infectious Diseases* **5**, 95 (1999).
- [3] G. Abramson, V.M. Kenkre, *Phys. Rev. E* **66**, 011912 (2002).
- [4] G. Abramson, V.M. Kenkre, T.L. Yates, R.R. Parmenter, *Bull. Math. Biol.* **65**, 519 (2003).
- [5] V. M. Kenkre, in *Modern Challenges in Statistical Mechanics: Patterns, Noise, and the Interplay of Nonlinearity and Complexity*, edited by V.M. Kenkre, K. Lindenberg, AIP Conf. Proc. No. 658, 63 (AIP, Melville, NY, 2003).
- [6] V.M. Kenkre, *Physica A* **342**, 242 (2004).
- [7] V.M. Kenkre, R.R. Parmenter, I. Peixoto, and L. Sadasiv, *Mathematical and Computer Modeling*, **42**, 313 (2005).
- [8] J. Ziman, *Electrons and Phonons: the Theory of Transport Phenomena in Solids*, 2nd edition (Oxford University Press, New York, 1960); M. Born and R. Oppenheimer, *Ann. Phys.* **84**, 457 (1927);
- [9] A. Okubo, *Diffusion and Ecological Problems: Modern Perspectives*, 2nd. edition (Springer-Verlag, Berlin,1980).
- [10] J.D. Murray, *Mathematical Biology*, 2nd edition (Springer-Verlag, New York, 1993).
- [11] M.A. Aguirre, G. Abramson, A.R. Bishop, and V.M. Kenkre, *Phys. Rev. E* **66**, 041908 (2002).
- [12] C. Escudero, J. Buceta, F.J. de la Rubia, and K. Lindenberg, *Phys. Rev. E* **70**, 061907 (2004).
- [13] M. Ballard, V.M. Kenkre, and M.N. Kuperman, *Phys. Rev. E* **70**, 031912 (2004).
- [14] C. Escudero, J. Buceta, F.J. de la Rubia, and K. Lindenberg, *Phys. Rev. E* **69**, 021908 (2004).
- [15] L. Giuggioli, V.M. Kenkre, *Physica D* **183**, 245 (2003).
- [16] V.M. Kenkre, M.N. Kuperman, *Phys. Rev. E* **67**, 51921 (2003).
- [17] L. Giuggioli, G. Abramson, V.M. Kenkre, G. Suzán, E. Marcé, T.L. Yates, *Bull. Math. Biol.* **67**, 1135 (2005).
- [18] G. Abramson, L. Giuggioli, V.M. Kenkre, J.W. Dragoo, R.R. Parmenter, C.A. Parmenter, T.L. Yates, *Ecol. Complexity* accepted for publication (2005).

- [19] L. Giuggioli, G. Abramson, V.M. Kenkre, R.R. Parmenter, and T.L. Yates, *J. Theor. Biol.* (2005) in press.
- [20] R.R. Parmenter, J.A. MacMahon, *Oecologia* **59**, 145 (1983).
- [21] L.F. Stickel, *Biology of Peromyscus (Rodentia)*, edited by J.A. King, Special Publication No. 2, p. 373 (The American Society of Mammalogists, Stillwater, OK, 1968).
- [22] J.O. Wolff, *J. Animal Ecol.* **66**,1 (1997).
- [23] V.M. Kenkre, *Physica A* **356**, 121 (2005).
- [24] D. MacInnis, G. Abramson and V. M. Kenkre, in preparation.
- [25] V.M. Kenkre and L. Giuggioli, in preparation.
- [26] E.W. Montroll and B. West, *J. Stat. Phys.* **13**, 17 (1975) and references therein.
- [27] A.T.C. Silva, G. Camelo-Neto, L. Giuggioli and V.M. Kenkre, University of New Mexico preprint.
- [28] M. Kac, in *3rd Berkeley Symposium on Mathematical Statistics, University of California* 171 (1956); E.W. Montroll, in *Energetics of Metallurgic Phenomena* (Gordon and Breach, New York, 1967), Vol. 3.
- [29] V.M. Kenkre and H.M. Van Horn, *Phys. Rev. A* **23**, 3200 (1981).
- [30] V. M. Kenkre and P. Reineker, *Exciton Dynamics in Molecular Crystals and Aggregates* (Springer-Verlag, Berlin, 1982).
- [31] M. Pope and C.E. Swenberg, *Electronic Processes in Organic Crystals and Polymers* (Oxford, New York, 1999).
- [32] M.V. Smoluchowski, *Phys. Z* **17**, 557 (1916); S. Chandrasekar, *Rev. Mod. Phys.* **15**, 1 (1943).
- [33] R. Durrett and S.A. Levin, *Phil. Trans. R. Soc. Lond. B* **343**, 329 (1994); R.S. Cantrell and C. Cosner, *Spatial Ecology via Reaction-Diffusion Equations* (John Wiley & Sons, 2003).
- [34] M.-Th. Hütt and R. Neff, *Physica A* **289**, 498 (2001).